

## **6. Varilux 1, the first commercial progressive lens**

### **The situation before the breakthrough by Bernard Maitenaz**

In a first patent filed in 1932 (US 2 001 952) Henry James Birchall specifies ( a little vaguely) a surface of the Rüssel type (elephant's trunk) and outlines briefly a manufacturing method for a progressive lens (not part of the claims). In a second patent filed in 1945 (US 2 475 275) he describes qualitatively how the curvature of the orthogonal sections has to evolve from the main meridian to the edge of the lens in order to reduce the lateral distortion. Bennett [1] presents sketches of an unpublished manuscript from H.J. Birchall showing how the deformation of a rectangular grid is getting smaller when the curvature of the sections perpendicular to the main meridian decreases to the edge of the lens (convex progressive surface) . A second claim covers a lens in which a progressive surface merges into a spherical section at either one or both ends. C.W. Kanolt in his patent US 2 878 721 (application 1954) gives a mathematical description of special progressive surfaces which are calculated to respect certain thresholds of peripheral astigmatism less than 1 D. The surface is divided into different areas described mathematically by polynomials. On the straight dividing lines of these areas the functions and their first and second derivatives have identical values. The power increases continuously from the top to the bottom of the lens and consequently there are no zones exempt from astigmatism.

So up to the fifties certain basic elements characterizing the structure and the performance of progressives were known, but the patents remain (almost exclusively) focussed on theoretical considerations of the surface geometry and image quality and do not address the problem how to realize the lens.

### **6.1 Focus on the manufacturing process**

It was the breakthrough for the progressive lens type when Bernard Maitenaz invented the technical means to produce economically a complex surface with no rotational symmetry. Already in his first patent US 2 869 422, filed November 25, 1953 in France he defined a progressive lens together with a detailed proposal for first manufacturing methods.

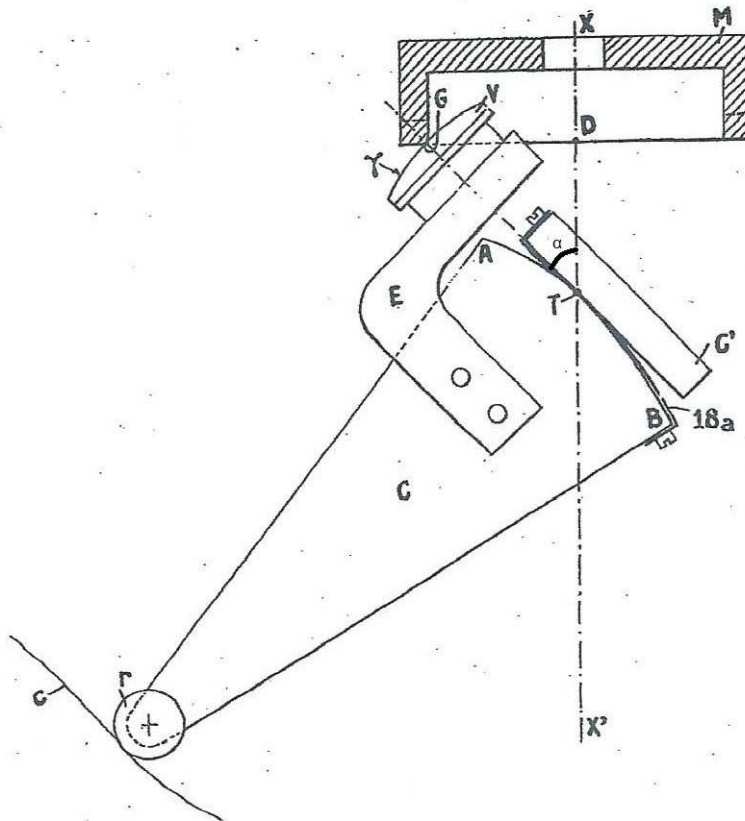


Fig 1

He describes a progressive design characterized by an umbilical line and a circle as the generatrix curve. In Fig 1 the generating surface (here reduced to a circle) is constituted by the circular edge of the inverted cup-grinding wheel. The evolute of the main meridian  $\gamma$  is the contour AB of the cam C, which is fixed to the mounting E of the lens V to be cut. This cam is rolling without slipping on the plane surface of the bar C'. A steel strip 18a ensures the slip-free rolling of the cams C and C' with a contact point T. The bar C' is mounted so, that it can pivot about a tangent perpendicular to the plane of the figure in the point G of the circular edge of the grinding tool. Following the theorem of Meusnier at point G the radius of curvature of the orthogonal section of the generated surface is given by

$$R_{os} = GD / \sin \alpha$$

where  $\alpha$  is the angle between the tool rotation axis and the normal to the main meridian in G.

The slip-free rolling motion of the cams C and C' takes place about a momentary rotation axis perpendicular to the plane of the figure in the contact point T between the two cams. So the radius of curvature  $R_d$  of the directrix, i.e. the main meridian, is TG, which is tangent to the evolute AB.

To make sure to get an umbilical line . i.e.  $Ros=Rd$  the contact point T between C and C' has always to lie on the rotation axis XX' of the grinding wheel. So there is a roller fixed to the cam C which rolls on another fixed cam c having a profile so designed, that the contact point T always will be maintained on the axis XX'.

In 1959 Bernard Maitenaz patented as US 2 915 856 "Machine for Grinding an Optical Surface in a Piece of Refractive Material" several manufacturing methods for more complex surfaces than that created by the generating surface of a circle described in the first patent.

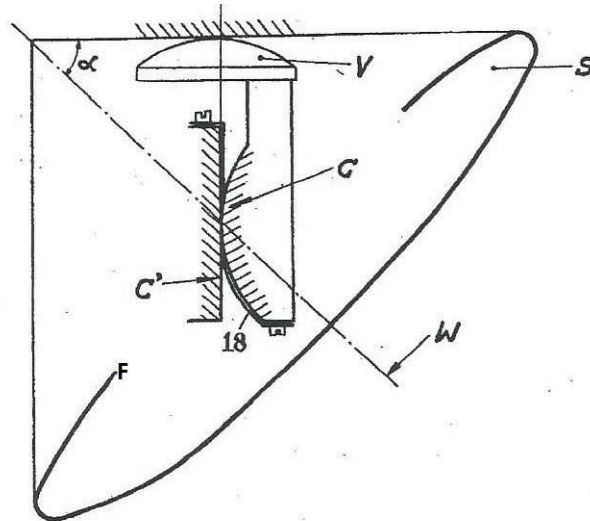


Fig 2

For example in Fig 2 the generating surface S is a cone of revolution with an half-angle  $\alpha$ . The cam C, fixed to the mounting of the lens is rolling without slipping on a vertical guide strip C'. The profile of the cam C is the involute of the main meridian to be cut. The steel strip 18 ensures the slip-free rolling motion. If the half-angle is  $45^\circ$  the sections perpendicular to the directrix of the generated surface are parabolas, changing for  $\alpha < 45^\circ$  into ellipses and into hyperbolas for  $\alpha > 45^\circ$ .

### Getting rid of the constraints: The point by point manufacturing

In his patent US 2 982 058 granted in 1961 Maitenaz describes the manufacturing method point by point with which he gets rid of all the constraints of the manufacturing methods using mechanical cams. This new method allows not only to realize the principal meridian with stabilized power sections for far and near vision but also to model the lateral parts in order to minimize the aberrations. This manufacturing method was the predecessor of to-days surface manufacturing with CNC machines. At the time of the Varilux creation the manufacture of a "point by point" surface with 4000 points with a 1 mm spacing lasted about 2 days.

The history of this era of development is described by Maitenaz in "Four steps that led to Varilux" [2] and is told by Jean-Charles Le Roux [3]. The long manufacturing time made it necessary to cut at first a master in metal which in a second step served as model for large scale copying on glass lenses (US patent 3 041 789).

Bernard Maitenaz describes how in the beginning of the Varilux creation the meridian chosen was of the type close to the involute of a circle and the astigmatism plot of these first designs are depicted in [2] as well as in figure 3 of the patent US 3 687 528 (the "Varilux 2" patent). These diagrams are similar to the plot which we calculated in the chapter "The Rüssel", where we made the same choice for the principal meridian. In the following years between 1951 and 1958 applying the "point by point" manufacturing method the meridian evolved to a curve with stabilized power for far and near vision and a surface design with large aberrationfree zones for far and near vision.

In 1959 the Société des Lunetiers successfully launched Varilux - the first commercial progressive lens.

## 6.2 The coordinate system

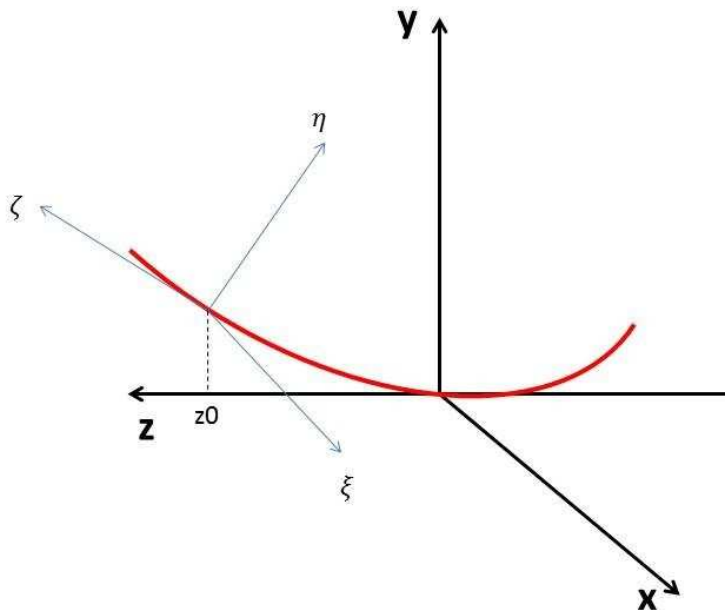


Fig 3

The main meridian is situated in the  $yz$  plane of a Cartesian coordinate system  $(x,y,z)$ . Moving from near vision to far vision  $z$  increases, the  $z$ -axis being tangent to a point in between (for example the center of the finished lens where the prismatic effect is checked).

The orthogonal sections are described in a Cartesian coordinate system  $(\xi,\eta,\zeta)$  moving with the orthogonal section. Where the section intersects the main meridian is the origin of this coordinate system, the  $\zeta$ -axis being tangent to the principal meridian, increasing  $\zeta$  meaning increasing  $z$ . So in this system the orthogonal section is described by an equation between  $\xi$  and  $\eta$ ,  $\xi$ - and  $x$ -values are identical.

### 6.3 The principal meridian

For a design with an umbilical main meridian and circular orthogonal sections (what we assume for the calculations), the power profile of the main meridian is the only degree of freedom. There were no precise data about the the Varilux 1 progression available. In [2] there is a diagram of the power progression with stabilized far and near vision zones and a length of about 12mm.

Fig 4 a and 4 b show two types of the main meridian with stabilized power regions, which we have tested here.

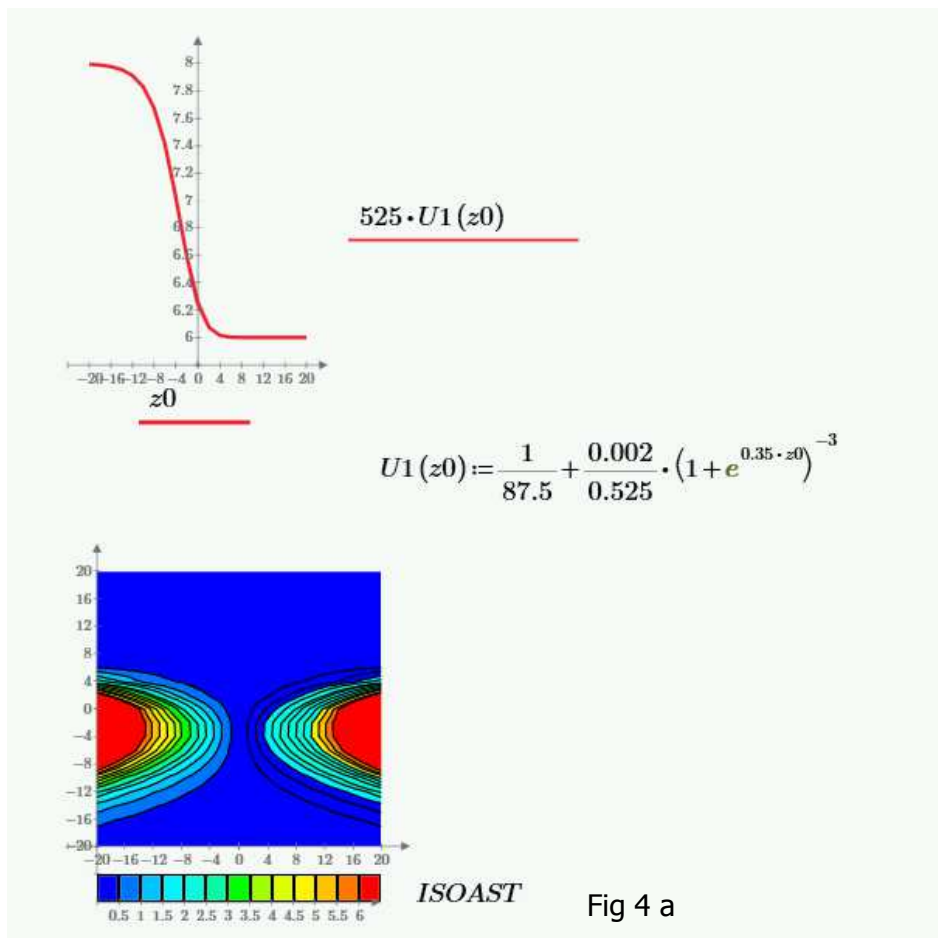


Fig 4 a

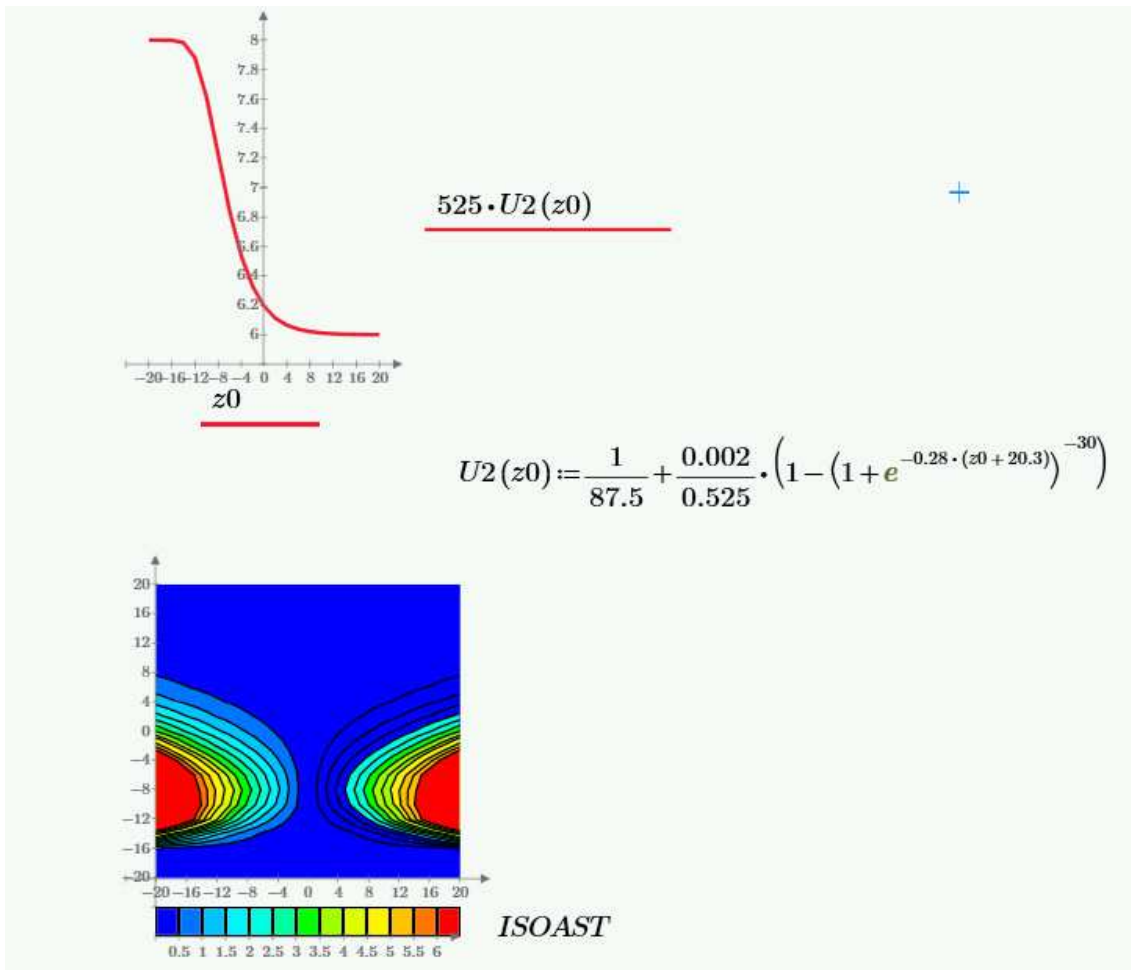


Fig 4 b

Both meridians have an effective progression length of 13 mm defined by the distance of the two meridian points with (FV power +0.12 D) and (NV power -0.12 D). For the meridian in Fig 4 a the transition into the power stabilization is more abrupt for the FV part than for the NV region, for the curve in Fig 4 b it is the opposite. Thus the first design shows a strong astigmatism gradient in the beginning of the far vision zone, the same is true for the second design as regards the upper lateral near vision region. A solution which maintains a short power progression, a widely aberrationfree FV and a reasonably broad NV, but has a more balanced astigmatism gradient, is represented by the following equation.

$$K(z_0) := \frac{1}{87.5} + \frac{0.0022}{4 \cdot 0.525} \cdot \left( 1 + 3 \cdot \left( 1 + e^{-0.29 \cdot (-z_0 - 3)} \right)^{-3} - \left( 1 + e^{-0.20 \cdot (z_0 + 28)} \right)^{-30} \right)$$

Nevertheless, also this design is a compromise, because the meridian shows a slight overpowering in the near vision part.

It has to be noted that  $K(z_0)$  is the geometrical curvature, multiplication with  $(n-1)$  gives the optical power. The far vision radius is 87.5 mm corresponding to the far vision power of 6 D. The add power is 2 D.

The main meridian  $Fm(z_0)$  and its first derivative are obtained by integration of the differential equation for the curvature.

### Integrating the differential equation for the curvature $K(z_0)$ of the meridian with power stabilization

$$\frac{Fm''(z_0)}{(1 + Fm'(z_0)^2)^{\frac{3}{2}}} = K(z_0) \quad Fm(z_0) = x_1(z_0)$$

$$x_1'(z_0) = x_2(z_0)$$

$$x_2'(z_0) = K(z_0) \cdot (1 + x_2(z_0)^2)^{\frac{3}{2}}$$

$$K(z_0) := \frac{1}{87.5} + \frac{0.0022}{4 \cdot 0.525} \cdot \left( 1 + 3 \cdot (1 + e^{0.29 \cdot (z_0 + 3)})^{-3} - (1 + e^{-0.20 \cdot (z_0 + 28)})^{-30} \right)$$

$$D(z_0, X) := \begin{bmatrix} X_1 \\ \frac{3}{2} \\ \left( 1 + X_1^2 \right) \cdot K(z_0) \end{bmatrix}$$

$$X(z_0) = \begin{bmatrix} x_1(z_0) \\ x_2(z_0) \end{bmatrix}$$

$$u := 3.689 \quad v := 0.3000$$

u and v are the initial values for  $F_m(z_0)$  and  $D1F_m(z_0)=F_m'(z_0)$  in  $z_0=25$  mm calculated first from a circle with  $r_f=87.5$ mm and then iteratively corrected, so that for  $z_0=0$   $F_m(z_0)$  and  $D1F_m(z_0)$  are zero

$$init := \begin{bmatrix} u \\ v \end{bmatrix}$$

$$Zi := 25$$

$$Zf := -25$$

$$N := 100$$

$$sol := \text{AdamsBDF}(init, Zi, Zf, N, D)$$

	$z_0$	$x_1=F_m$	$x_2=F_m'(z_0)$
$sol =$	$2.5 \cdot 10^{-1}$	3.689	$3 \cdot 10^{-1}$
	$2.45 \cdot 10^{-1}$	3.541	$2.935 \cdot 10^{-1}$
	$2.4 \cdot 10^{-1}$	3.395	$2.871 \cdot 10^{-1}$
	$2.35 \cdot 10^{-1}$	3.254	$2.806 \cdot 10^{-1}$
			$\vdots$

### Calculating the main meridian as a function of $z_0$ : $F_m(z_0)$

Arranging the data in an ascending order of t

$$data := \text{csort}(sol, 0)$$



$$data = \begin{bmatrix} -25 & 4.319 & -0.379 \\ -24.5 & 4.132 & -0.37 \\ -24 & 3.949 & -0.36 \\ -23.5 & 3.771 & -0.351 \\ -23 & 3.598 & -0.342 \\ -22.5 & 3.429 & -0.333 \\ -22 & 3.265 & -0.324 \\ -21.5 & 3.106 & -0.315 \\ -21 & 2.951 & -0.306 \\ -20.5 & 2.8 & -0.297 \\ & & \vdots \end{bmatrix}$$

$$Z := data^{(0)} \quad X1 := data^{(1)} \quad X2 := data^{(2)}$$

$$S1 := cspline(Z, X1)$$

$$Fm(z0) := interp(S1, Z, X1, z0)$$

$$S2 := cspline(Z, X2)$$

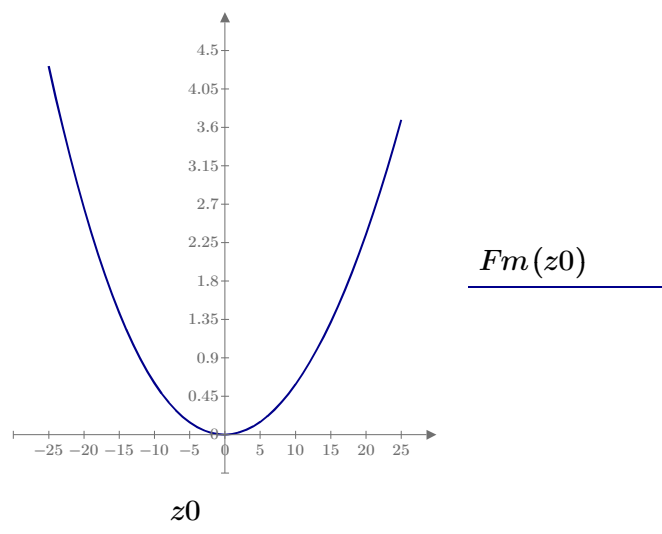
$$z0 := -25, -24..25$$


Fig 5

$$D1Fm(z_0) := \text{interp}(S2, Z, X2, z_0)$$

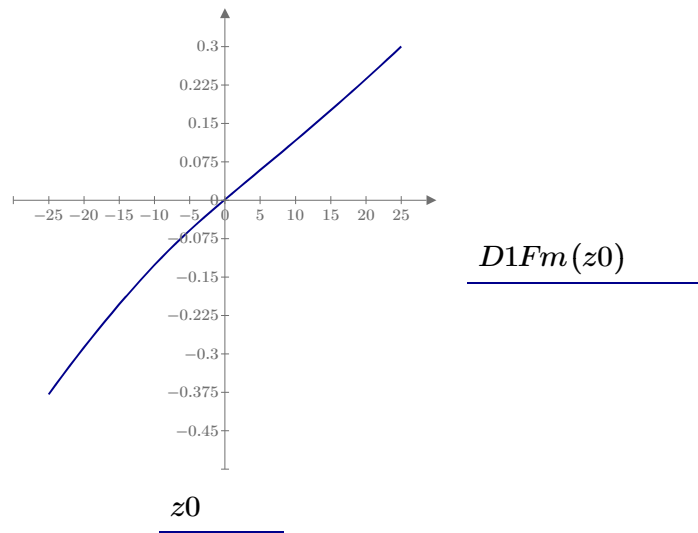


Fig 6

## 6.4 Geometry and equations of the progressive surface

Assuming that the orthogonal sections are circles with radii of curvature which are respectively equal to the radii of curvature of the meridian at the points of intersection (umbilical line), the vertex equation of the circle is

$$\eta(z_0, \xi) := \frac{\left(1 - \sqrt{1 - \xi^2 \cdot K(z_0)^2}\right)}{K(z_0)}$$

So in the  $(x, y, z)$ -coordinate system we get

$$x(z_0, \xi) := \xi$$

$$y(z_0, \xi) := Fm(z_0) + \frac{\eta(z_0, \xi)}{\sqrt{1 + D1Fm(z_0)^2}}$$

$$z(z_0, \xi) := z_0 - \eta(z_0, \xi) \cdot \frac{D1Fm(z_0)}{\sqrt{1 + D1Fm(z_0)^2}}$$

### 6.4.1 Fundamental Forms

Definitions

$$r(z_0, \xi) := \begin{bmatrix} x(z_0, \xi) \\ y(z_0, \xi) \\ z(z_0, \xi) \end{bmatrix}$$

$$xz_0(z_0, \xi) := \frac{d}{dz_0} x(z_0, \xi)$$

$$yz_0(z_0, \xi) := \frac{d}{dz_0} y(z_0, \xi)$$

$$zz_0(z_0, \xi) := \frac{d}{dz_0} z(z_0, \xi)$$

$$rz_0(z_0, \xi) := \begin{bmatrix} xz_0(z_0, \xi) \\ yz_0(z_0, \xi) \\ zz_0(z_0, \xi) \end{bmatrix}$$

$$x\xi(z_0, \xi) := \frac{d}{d\xi} x(z_0, \xi)$$

$$y\xi(z_0, \xi) := \frac{d}{d\xi} y(z_0, \xi)$$

$$z\xi(z_0, \xi) := \frac{d}{d\xi} z(z_0, \xi)$$

$$r_{\xi}(z_0, \xi) := \begin{bmatrix} x_{\xi}(z_0, \xi) \\ y_{\xi}(z_0, \xi) \\ z_{\xi}(z_0, \xi) \end{bmatrix}$$

$$xz_0z_0(z_0, \xi) := \frac{d^2}{dz_0^2} x(z_0, \xi)$$

$$yz_0z_0(z_0, \xi) := \frac{d^2}{dz_0^2} y(z_0, \xi)$$

$$zz_0z_0(z_0, \xi) := \frac{d^2}{dz_0^2} z(z_0, \xi)$$

$$r_{z_0z_0}(z_0, \xi) := \begin{bmatrix} xz_0z_0(z_0, \xi) \\ yz_0z_0(z_0, \xi) \\ zz_0z_0(z_0, \xi) \end{bmatrix}$$

$$x_{\xi\xi}(z_0, \xi) := \frac{d^2}{d\xi^2} x(z_0, \xi)$$

$$y_{\xi\xi}(z_0, \xi) := \frac{d^2}{d\xi^2} y(z_0, \xi)$$

$$z_{\xi\xi}(z_0, \xi) := \frac{d^2}{d\xi^2} z(z_0, \xi)$$

$$r_{\xi\xi}(z_0, \xi) := \begin{bmatrix} x_{\xi\xi}(z_0, \xi) \\ y_{\xi\xi}(z_0, \xi) \\ z_{\xi\xi}(z_0, \xi) \end{bmatrix}$$

$$xz_0\xi(z_0, \xi) := \frac{d}{d\xi} \left( \frac{d}{dz_0} x(z_0, \xi) \right)$$

$$yz_0\xi(z_0, \xi) := \frac{d}{d\xi} \left( \frac{d}{dz_0} y(z_0, \xi) \right)$$

$$zz_0\xi(z_0, \xi) := \frac{d}{d\xi} \left( \frac{d}{dz_0} z(z_0, \xi) \right)$$

$$r_{z_0\xi}(z_0, \xi) := \begin{bmatrix} x_{z_0\xi}(z_0, \xi) \\ y_{z_0\xi}(z_0, \xi) \\ z_{z_0\xi}(z_0, \xi) \end{bmatrix}$$

### 1. Fundamental Form and unit normal vector

$$E(z_0, \xi) := r_{z_0}(z_0, \xi) \cdot r_{z_0}(z_0, \xi)$$

$$F(z_0, \xi) := r_{z_0}(z_0, \xi) \cdot r_{\xi}(z_0, \xi)$$

$$G(z_0, \xi) := r_{\xi}(z_0, \xi) \cdot r_{\xi}(z_0, \xi)$$

$$N_o(z_0, \xi) := \frac{r_{z_0}(z_0, \xi) \times r_{\xi}(z_0, \xi)}{\|r_{z_0}(z_0, \xi) \times r_{\xi}(z_0, \xi)\|}$$

### 2. Fundamental Form

$$L(z_0, \xi) := r_{z_0 z_0}(z_0, \xi) \cdot N_o(z_0, \xi)$$

$$M(z_0, \xi) := r_{z_0 \xi}(z_0, \xi) \cdot N_o(z_0, \xi)$$

$$N(z_0, \xi) := r_{\xi \xi}(z_0, \xi) \cdot N_o(z_0, \xi)$$

$$H1(z_0, \xi) := E(z_0, \xi) \cdot N(z_0, \xi) + G(z_0, \xi) \cdot L(z_0, \xi) - 2 \cdot F(z_0, \xi) \cdot M(z_0, \xi)$$

$$H2(z_0, \xi) := E(z_0, \xi) \cdot G(z_0, \xi) - F(z_0, \xi)^2$$

$$H3(z_0, \xi) := L(z_0, \xi) \cdot N(z_0, \xi) - M(z_0, \xi)^2$$

Principal curvatures

$$K1(z0, \xi) := \frac{\left( H1(z0, \xi) + \sqrt{\left( H1(z0, \xi)^2 - 4 H2(z0, \xi) \cdot H3(z0, \xi) \right)} \right)}{2 \cdot H2(z0, \xi)}$$

$$K2(z0, \xi) := \frac{\left( H1(z0, \xi) - \sqrt{\left( H1(z0, \xi)^2 - 4 H2(z0, \xi) \cdot H3(z0, \xi) \right)} \right)}{2 \cdot H2(z0, \xi)}$$

#### 6.4.2 Mean optical power POW and Astigmatism AST

$$POW(z0, \xi) := 525 \cdot \frac{(K1(z0, \xi) + K2(z0, \xi))}{2}$$

$$AST(z0, \xi) := 525 \cdot (K1(z0, \xi) - K2(z0, \xi))$$

Check, that the principal meridian is an umbilical line

$$\xi := 0$$

$$z0 := -25, -20 \dots 25$$

$$AST(z0, \xi) = \begin{bmatrix} 0.003 \\ 8.14 \cdot 10^{-6} \\ 5.626 \cdot 10^{-4} \\ 4.089 \cdot 10^{-5} \\ 0.002 \\ 2.834 \cdot 10^{-4} \\ 1.873 \cdot 10^{-4} \\ 6.137 \cdot 10^{-5} \\ 3.447 \cdot 10^{-5} \\ 6.843 \cdot 10^{-6} \\ 0.002 \end{bmatrix} \quad POW(z0, \xi) = \begin{bmatrix} 8.19 \\ 8.163 \\ 7.992 \\ 7.444 \\ 6.576 \\ 6.1 \\ 6.023 \\ 6.008 \\ 6.003 \\ 6.001 \\ 5.999 \end{bmatrix}$$

**Lines of constant mean optical power (Isopowerlines )**

Loop calculation

$$\xi_{min} := -20 \quad \xi_{max} := 20 \quad n := 20 \quad i := 0 .. n$$

$$\Delta\xi := \frac{\xi_{max} - \xi_{min}}{n} \quad \xi_i := \xi_{min} + i \cdot \Delta\xi$$

$$z0_{min} := -20 \quad z0_{max} := 20$$

$$\Delta z0 := \frac{z0_{max} - z0_{min}}{n} \quad z0_i := z0_{min} + i \cdot \Delta z0$$

```

MPOW( $\xi$ , z0) := || for i  $\in$  0 .. last( $\xi$ )
|| || for j  $\in$  0 .. last(z0)
|| || || MPowi,j  $\leftarrow$  POW(z0j,  $\xi$ i)
|| || || Mzi,j  $\leftarrow$  z0j
|| || || Mxi,j  $\leftarrow$  x(z0j,  $\xi$ i)
|| || ||
|| return [ Mx ]
|| || [ Mz ]
|| || [ MPow ]
||

```

$$ISOPOW := MPOW(\xi, z0) = \begin{bmatrix} [21 \times 21] \\ [21 \times 21] \\ [21 \times 21] \end{bmatrix}$$

Mathcad program

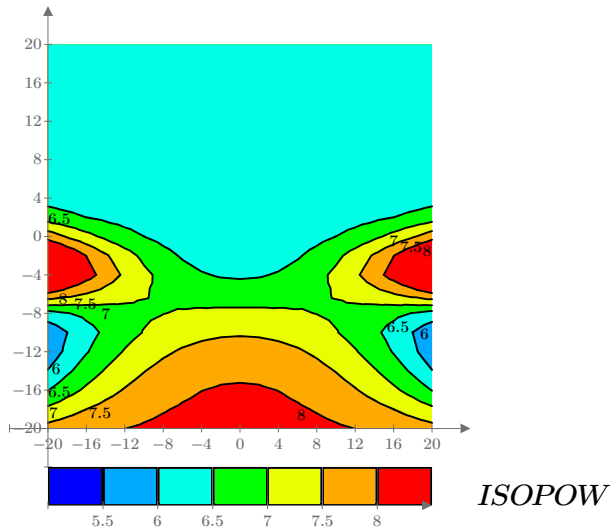
*For the calculation of the isolines-pattern the proposed Mathcad-function FA works only if the absolute-sign is used. Possibly during the iteration process complex numbers occur.*

$$FA(\xi, z0) := \|POW(z0, \xi)\|$$

$$\xi_{low} := -20 \quad \xi_{high} := 20 \quad \xi_n := 20$$

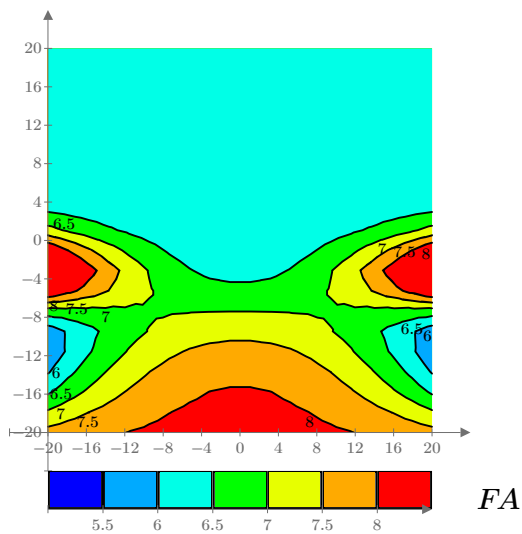
$$z0_{low} := -20 \quad z0_{high} := 20 \quad z0_n := 20$$

$$FA := CreateMesh(FA, \xi_{low}, \xi_{high}, z0_{low}, z0_{high}, \xi_n, z0_n)$$



Loop calculation

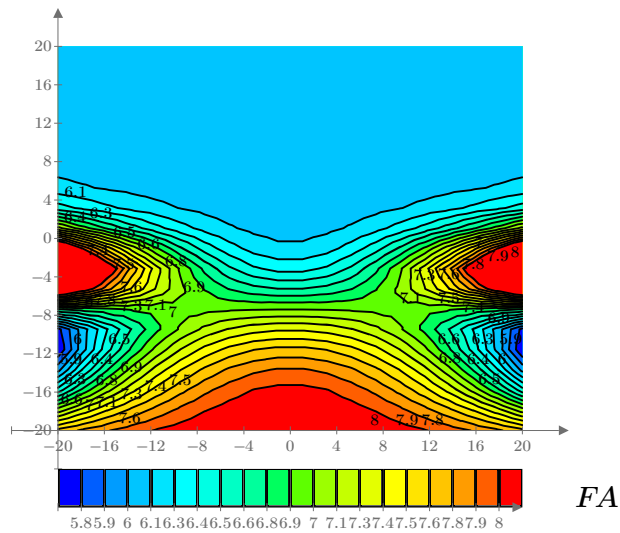
Fig 7



Mathcad program



Power increase in 0.125-steps



Mathcad program

Fig 7 a

### Lines of constant astigmatism (Isoastigmatism plot)

Loop calculation

$$\xi_{min} := -20 \quad \xi_{max} := 20 \quad n := 20 \quad i := 0..n$$

$$\Delta\xi := \frac{\xi_{max} - \xi_{min}}{n} \quad \xi_i := \xi_{min} + i \cdot \Delta\xi$$

$$z0_{min} := -20 \quad z0_{max} := 20$$

$$\Delta z0 := \frac{z0_{max} - z0_{min}}{n} \quad z0_i := z0_{min} + i \cdot \Delta z0$$

$$\begin{aligned}
 MAST(\xi, z0) := & \begin{array}{l}
 \text{for } i \in 0 \dots \text{last}(\xi) \\
 \quad \text{for } j \in 0 \dots \text{last}(z0) \\
 \quad \quad MAsti_{i,j} \leftarrow AST(z0_j, \xi_i) \\
 \quad \quad Mz_{i,j} \leftarrow z0_j \\
 \quad \quad Mx_{i,j} \leftarrow x(z0_j, \xi_i) \\
 \quad \quad \quad \left[ \begin{array}{c} Mx \\ Mz \\ MAsti \end{array} \right] \\
 \text{return} \left[ \begin{array}{c} Mx \\ Mz \\ MAsti \end{array} \right]
 \end{array}
 \end{aligned}$$

$$ISOAST := MAST(\xi, z0) = \begin{bmatrix} [21 \times 21] \\ [21 \times 21] \\ [21 \times 21] \end{bmatrix}$$

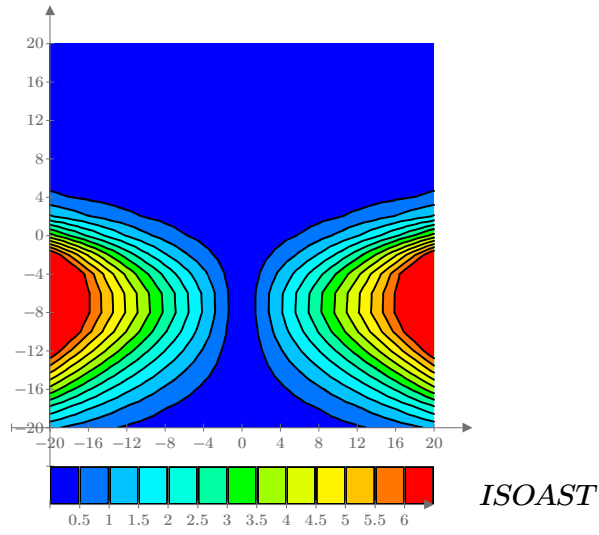
Mathcad program

$$FA(\xi, z0) := \|AST(z0, \xi)\|$$

$$\xi_{low} := -20 \quad \xi_{high} := 20 \quad \xi_n := 20$$

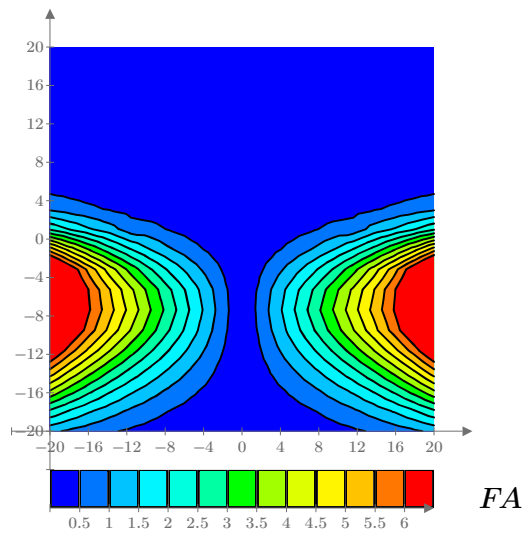
$$z0_{low} := -20 \quad z0_{high} := 20 \quad z0_n := 20$$

$$FA := \text{CreateMesh}(FA, \xi_{low}, \xi_{high}, z0_{low}, z0_{high}, \xi_n, z0_n)$$



Loop calculation

Fig 8



Mathcad program

## 6.5 Analysis of design and calculations

For the calculations of this document circles were chosen as orthogonal sections, as it was claimed for the first Varilux in the commercial publications. Maitenaz also speaks in his famous Varilux 2- patent US 3 687 528 of circles as the sections of the first surfaces. The Isopower- and Isoastigmatism-plots Fig 7 and 8 show large viewing zones for far- and near-vision. Rather nice are the almost horizontal isopower-lines. The effective progression length measured between the points where the meridian power reaches 6.12 respectively 7.88 D is about 14 mm ( see power plot 6 a in 0.125 steps).

In the periphery the power progression shows respectively two symmetrically situated "islands" of steeper increase in the upper part of the progression and of power decrease in the lower part.

The lateral astigmatism increases strongly towards the periphery and reaches values for more than 6 D (which is more than 3 x add power) for  $x > 16$  mm.

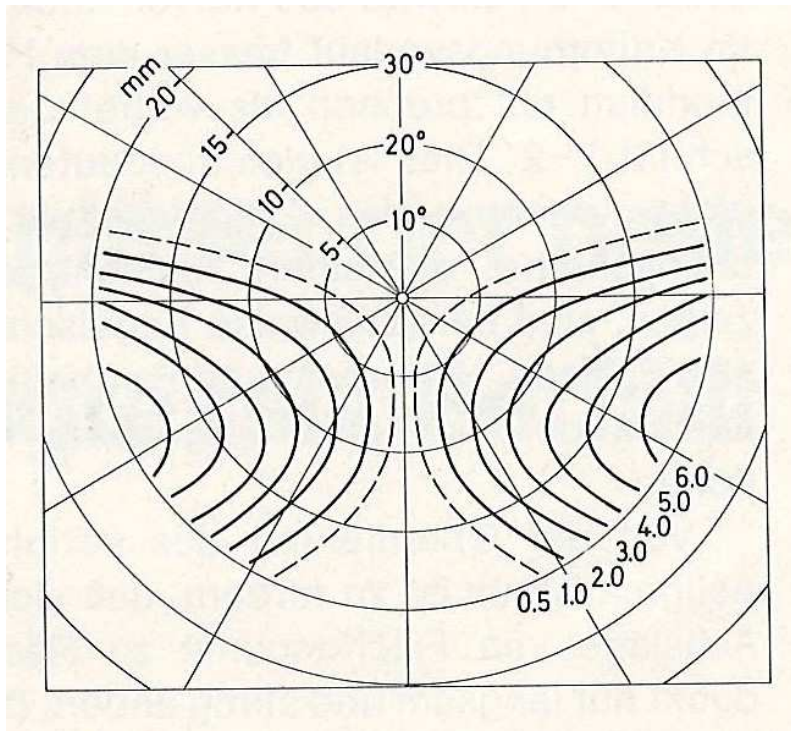


Fig 9

The design shown in Fig 9 is not the Varilux 1, but another design of the first generation which was launched in 1974 by BBGR, France, under the tradename Zoom [4]. As regards the pattern of the isolines and the maximum value of the lateral astigmatism it is close to the design calculated in this chapter. The Zoom design is a little softer and its astigmatism gradient is a little more shifted downwards. So as already mentioned, the meridian in 6.3 is not yet the optimum.

The lateral aberrations of this first progressive design required from the wearer a certain adaptation time to these new lenses, sometimes lasting several days . One special optical effect was the distortion of vertical and horizontal lines of the objects , particularly disturbing under dynamic viewing conditions , i.e. either when the wearer had to turn his head fixing an object with his eyes or when he followed with his eyes a moving object.

This was a drawback of the development goal to keep the Varilux 1 design close to the characteristics of a bifocal, where the far vision part was entirely exempt from aberrations and the progression was modeling only the lower half of the lens.

In the next step of his invention Maitenaz extended the aspherical design to the totality of the lens surface .

## **References**

1. A.G. Bennett: Variable and Progressive Power Lenses. Manufacturing Optics International, March 1973
2. Bernard Maitenaz: Four Steps that led to Varilux. Am. J. Optom., Vol. 43, 1966
3. Jean Charles Le Roux: L'épopée Varilux, editions Perrin, 2007
4. Werner Köppen: Progressive Brillengläser der neuen Generation, der Augentoptiker, no.4, 1980